13.9

THE MESOSCALE EVOLUTION OF THE EARLY CYCLOGENESIS OF THE MARCH 1993 STORM OF THE CENTURY

K. D. Pfeiffer, M. L. Kaplan, Y.-L. Lin[1], A. J. Riordan,
G. M. Lackmann, K. T. Waight III[2], D. B. Ensley
North Carolina State University, Raleigh, North Carolina

1. INTRODUCTION

Although considered largely a forecasting success, much of the early development of the March 1993 Storm of the Century (SOC93) was not captured in *any* operational model (Uccellini *et al.*, 1995). SOC93 formed initially in the western Gulf of Mexico under an intense mesoscale convective complex (MCC) early on 12 March (Fig. 1). Previous investigators have attributed the failure of operational forecasts in part to the inadequate simulation of this organized convection (Caplan, 1995; Dickinson *et al.*, 1997). Other studies have indicated that the poor initialization of the sea surface temperature (SST) field along the Texas Gulf Coast may have contributed to weaker and more poorly organized convection in operational forecasts (Gilhousen, 1994; Huo *et al.*, 1998).

Understanding how this MCC (Fig. 1) forms, then, is critical to understanding the nascent storm. Fundamentally, organized convection requires instability, moisture and a trigger. Previous investigators have implicated a mid-level cold pool oriented along the Texas Gulf Coast as the source of the convective available potential energy (CAPE) in the column (Gilhousen, 1994; Huo *et al.*, 1995; Bosart *et al.*, 1996; Dickinson *et al.*, 1997). We assert, however, that the *mesoscale* details of this phenomenon have not been elucidated. In this presentation, we employ observation and mesoscale simulation datasets to trace the origin of the mid-level cold pool that conditions the environment for deep convection in the period prior to 1200 UTC 12 March.

[1] Corresponding author: Prof. Yuh-Lang Lin, Department of Marine, Earth, and Atmospheric Sciences, North Carolina State University, Raleigh, North Carolina 27695-8208 e-mail: yl_lin@ncsu.edu
[2] MESO Inc., 1005 Capability Drive, Raleigh, North Carolina, 27695-8208

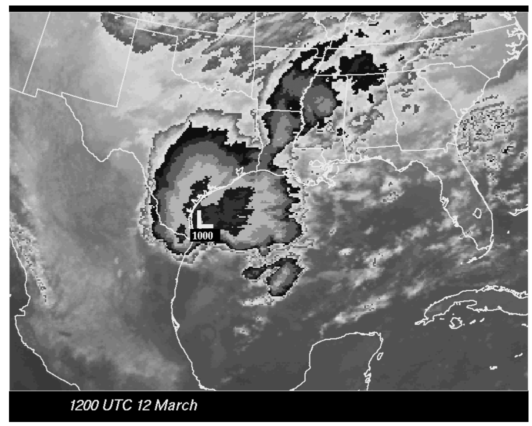

FIG. 1. GOES-7 IR imagery from 1200 UTC 12 March. Position of the surface low from the Kocin *et al.* (1995) mesoanalysis is indicated.

2. METHODOLOGY

Simulations were performed with the Mesoscale Atmospheric Simulation System (MASS) version 5.12 (MESO Inc., 1993) on a $260 \times 220 \times 45$ grid at 12 km horizontal resolution. The numerical experiments were initialized at 1200 UTC 10 March, or about 48 h prior to the formation of the surface cyclone, and integrated to 0000 UTC 14 March. European Center for Medium-range Weather Forecasts (ECMWF) uninitialized gridded analyses at 1.125° (T106) resolution were used as initial and boundary conditions for these simulations. Verification of the control simulation indicates a mean error in surface storm central pressure of +3.4 hPa and a mean position error of 109 km (Fig. 2), which is consistent with previous studies that have initialized at 0000 UTC 12 March or later (e.g. Huo *et al.*, 1998). The model domain is indicated by the boundaries in Fig. 2b. Further verification details are provided in Pfeiffer *et al.* (2001a, 2001b).

3. ORIGIN OF PRECURSOR CAPE

The MCC that formed the initial SOC93 erupted early on 12 March in an environment destabilized by a mid-level cold pool. This cold pool has been noted in previous studies (Huo *et al.*, 1995; Kocin *et al.*, 1995; Bosart *et al.*, 1996; Dickinson *et al.*, 1997) and is evident in the ECMWF analysis as a 700 hPa cold trough in the isentropes extending from central Texas to northeastern Mexico, just west of Brownsville (BRO), Texas, at 0000 UTC 12 March (Fig. 3a).

The impact of this cold feature on the lower troposphere can be measured with the convective available potential energy (CAPE) in the column (e.g. Emanuel, 1994, Sec. 6.3). The propagation of this cold air down the Rio Grande Valley decreases the environmental potential temperature (θ) through a significant layer (800 to 400 hPa), while near-surface flow from the Gulf of Mexico provides warm, moist (high θ_e) air, effectively increasing the available potential energy in the column. CAPE was calculated from ECMWF-derived soundings at BRO for the period 1200 UTC 10 March to 1200 UTC 13 March. A 72-h time series (Fig. 3b) shows a peak in CAPE just after 0000 UTC 12 March of about 1600 J kg^{-1}, coincident with the approach and passage of this mid-level cold pool.

Although there is a diurnal component to this maximum, we assert that it is of secondary importance to the sharp peak at 0000 UTC 12 March (Fig. 3b): surface temperatures at BRO on 11 March range from 68°F at midnight local to a daytime high of 78°F in the afternoon. Radiosonde data available every 12 h at BRO confirms the shape of the time series (Fig. 3b) though the similarity between the two is influenced in part by incorporation of radiosonde data into the ECMWF data assimilation cycle.

We contend that this meso-α scale cooling at 700 hPa (Fig. 3a) originates in the upper Rio Grande Valley near Del Rio (DRT), TX early on 11 March. The 0000 UTC 11 March sounding at DRT indicates a quasi-adiabatic layer from about 800 to 500 hPa (Fig. 4a) that originates on the central Mexican plateau (terrain indicated in Fig. 2b); this elevated mixed layer (EML) has been investigated by many authors, especially in relation to springtime convective events (e.g. Lanicci and Warner, 1997). This EML is transported north-

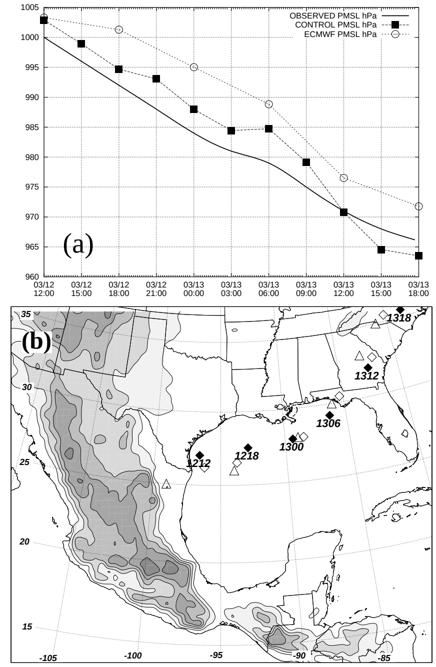

FIG. 2. Track of the SOC93 surface cyclone in the mesoanalysis of Kocin et al. (1995), the CONTROL simulation and the ECMWF analysis. Depicted are comparisons of (a) storm central pressures and (b) storm position, where the mesoanalysis is indicated by a filled diamond, the CONTROL simulation is indicated by a hollow diamond, and the ECMWF analysis is indicated by the hollow triangle. Times in (b) are of the form *DDHH* (e.g. 1218 = 1800 UTC 12 March); terrain height is shaded every 500 m.

ward by a large, thermally-direct mountain-plains solenoid (MPS). The 1200 UTC sounding at DRT indicates a cool, moist layer from about 850 to 750 hPa that appears to form at the junction of the EML and the boundary layer.

The control simulation at 0900 UTC 11 March yields insight into this cold pool, revealing a 500 km cold trough at 700 hPa southeast of DRT (Fig. 5a). A cross-section through this feature (Fig. 5c) shows that the cold pool forms over a narrow warming at about 800 hPa above near-surface cold air associated with a quasi-stationary surface front. This warming is consistent with the observed shift of winds in the cold pool from southwesterly to southerly (Fig. 4a). The southwesterly flow is associated with warm, dry MPS outflow from the Mexican plateau, while the south to southeasterly flow is associated with the transport of warm, moist air from the Gulf. The resulting cool, moist layer appears to be the prod-

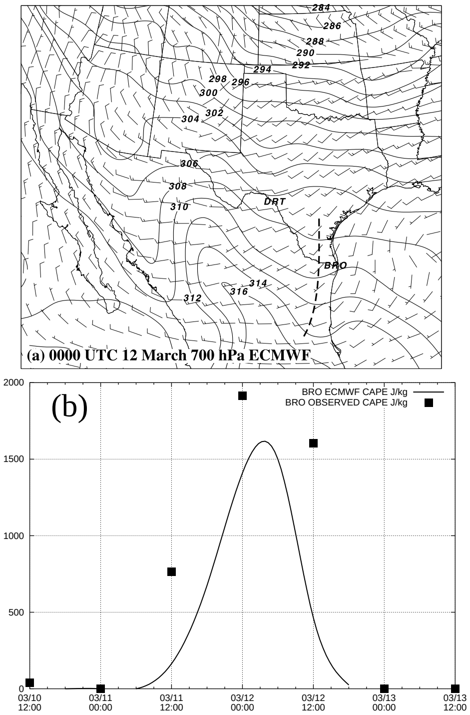

FIG. 3. ECMWF analysis (a) 700 hPa potential temperature field at 0000 UTC 12 March contoured every 1 K, with standard wind vectors in m s^{-1}. and (b) time-series plot of ECMWF-derived CAPE (in J kg^{-1}) at Brownsville (BRO), Texas, from 1200 UTC 10 March to 1200 UTC 13 March, with observed BRO CAPE values plotted with filled squares. The cold trough is denoted by the dashed line in (a).

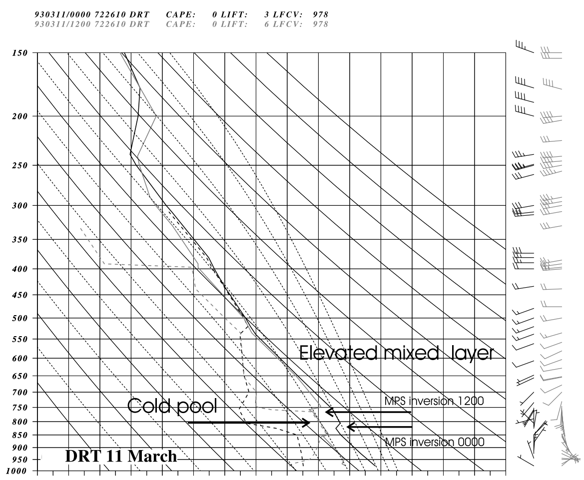

FIG. 4. Observed soundings at Del Rio (DRT), TX, at 0000 and 1200 UTC 11 March, temperature (solid) and dewpoint (dashed) in K, wind vectors in m s^{-1}, with 0000 sounding in black and 1200 in dark gray.

uct of both adiabatic cooling (ascent) and evaporational cooling from shallow convection triggered by this low-level warming. The signal of low-level warming appears to maximize about 850 hPa; note the sharp depression in the isentropes about midway through the cross-section in Fig. 5b at about 850 hPa. This is confirmed by computation of 850 hPa temperature advection on the simulation fields, indicating strong elevated warming (4 to 12 K 3 h^{-1}) along the eastern edge of the 700 hPa cold pool (Fig. 5c). This low-level warm advection up the Rio Grande Valley triggers shallow convection, indicated in both satellite (Fig. 5c) and simulated precipitation fields (Fig. 5a,b), consistent with the large-scale capping of the lower troposphere by the EML (Lanicci and Warner, 1991). The warm plume at 850 hPa is similar to but weaker than the springtime Brownsville jet investigated by Igau and Nielsen-Gammon (1998) and has been identified as the hot conveyor belt for this study (Pfeiffer *et al.*, 2001a).

Simulation results (not shown) indicate that the cold pool is initiated about 0600 UTC 11 March west of DRT. Once triggered, the cold pool continues to expand as the cycle of low-level warming triggering shallow convection produces evaporationally-cooled air in the layer between 800 and 600 hPa. Surface observations between DRT and Brownsville (BRO), TX, on 11 March show little precipitation, indicating that most of the moisture transported northward by the hot conveyor belt is used to produce the mid-level cool, moist layer. We speculate that this cold pool propagates down the Rio Grande Valley *in response to* the eastward progression of the hot conveyor belt. A similar phenomenon has been documented in an observational study of the dryline by Zeigler and Hane (1993).

Although the cold pool aloft should destabilize the lower troposphere, the surface temperatures are cool through much of the upper Rio Grande Valley because of the stagnant surface boundary. The observed CAPE at DRT remains zero despite the presence of this cool, moist layer (Fig. 4). By 0000 UTC 12 March, however, this cold pool is juxtaposed with the warm, moist lower troposphere of the Gulf Coast, destabilizing the genesis region of SOC93: the simulated (Fig. 6) and observed (Fig. 3a) cold pool both produce CAPE values $>$ 1000 J kg^{-1} proximal to BRO.

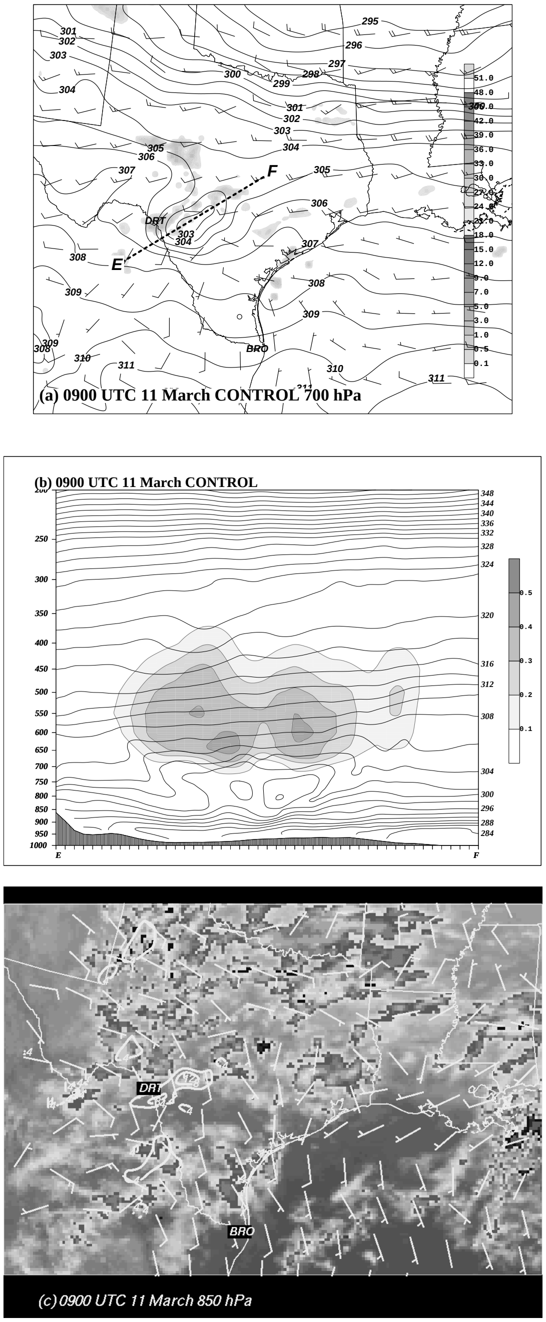

FIG. 5. CONTROL fields at 0900 UTC 11 March. (a) 700 hPa isentropes (contoured every 1 K), precipitation (mm h^{-1}), and wind vectors (m s^{-1}); (b) Cross-section, isentropes contoured every 2 K, and precipitation mixing ratio shaded every 0.1 g kg^{-1}; and (c) 850 hPa potential temperature advection ($-\mathbf{V} \bullet \nabla\theta$) contoured every 4 K 3 h^{-1}, positive (warm) advection only.

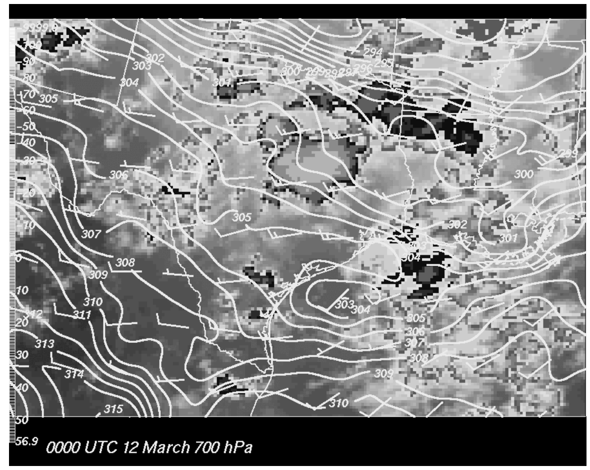

FIG. 6. CONTROL 700 hPa fields on GOES-7 IR at 0000 UTC 12 March. Depicted are isentropes contoured every 1 K and standard wind vectors in m s^{-1}.

4. CONCLUDING DISCUSSION

Mesoscale simulation results indicate that the source of initial convective available potential energy along the Texas Gulf Coast is developed in the upper Rio Grande Valley early on 11 March as a cold pool formed by evaporational cooling in a convectively unstable layer (about 800 hPa to 600 hPa). These results clarify previous studies which have speculated that this cold pool is produced in response to frontogenetic circulations confined to the western Gulf Coast, possibly enhanced by SST gradients along the coast. (Gilhousen, 1994; Bosart *et al.*, 1996; Dickinson *et al.*, 1997). Additional work with mesoscale simulations has been accomplished to document how this instability is triggered early on 12 March (Pfeiffer *et al.*, 2001b). Further work will study the overwater development of SOC93 from about 1200 UTC 12 March to 0600 UTC 13 March.

Acknowledgments The Air Force Combat Climatology Center, Asheville, NC, provided additional surface and upper air data over Mexico. Phil Schumacher supplied surface data from the Kocin *et al.* (1995) mesoanalysis, used in verification computations. Numerical simulations were executed on an SGI/Origin 2000 operated by the North Carolina Supercomputing Center (NCSC). This research was funded under NASA Grant NAG-5480C. The authors would like to acknowledge Dr. Ramesh Kakar, Manager, Atmospheric

Dynamics and Thermodynamics Program, NASA Headquarters, Washington, D.C. The views expressed in this article are those of the authors and do not reflect the official policy or position of the United States Air Force, Department of Defense or U.S. Government.

REFERENCES

Bosart, L. F., G. J. Hakim, K. R. Tyle, M. A. Bedrick, M. J. Dickinson, and D. M. Schultz, 1996: Large-scale antecedent conditions associated with the 12–14 March 1993 cyclone ("Superstorm 93") over eastern North America. *Mon. Wea. Rev.*, **124**, 1865–1891.

Caplan, P. M., 1995: The 12–14 March 1993 Superstorm: Performance of NCEP Global Medium Range Model. *Bull. Amer. Meteor. Soc.*, **76**, 202–212.

Dickinson, M. J., L. F. Bosart, W. E. Bracken, G. J. Hakim, D. M. Schultz, M. A. Bedrick, and K. R. Tyle, 1997: The March 1993 Superstorm cyclogenesis: Incipient phase synoptic- and convective-scale flow interaction and model performance. *Mon. Wea. Rev.*, **125**, 3041–3072.

Emanuel, K. A., 1994: *Atmospheric Convection*. Oxford University Press.

Gilhousen, D. B., 1994: The value of NDBC observations during March 1993's Storm of the Century. *Wea. Forecasting*, **9**, 255–264.

Huo, Z., D.-L. Zhang, and J. Gyakum, 1995: A diagnostic analysis of the Superstorm of March 1993. *Mon. Wea. Rev.*, **123**, 1740–1761.

Huo, Z., D.-L. Zhang, and J. Gyakum, 1998: An application of potential vorticity inversion to improving the numerical prediction of the March 1993 Superstorm. *Mon. Wea. Rev.*, **126**, 424–436.

Igau, R. C. and J. W. Nielsen-Gammon, 1998: Low-level jet development during a numerically simulated return flow event. *Mon. Wea. Rev.*, **126**, 2972–2990.

Kocin, P. J., P. N. Schumacher, R. F. Morales, and L. W. Uccellini, 1995: Overview of the 12–14 March 1993 Superstorm. *Bull. Amer. Meteor. Soc.*, **76**, 165–182.

Lanicci, J. M. and T. T. Warner, 1991: A synoptic climatology of the elevated mixed-layer inversion over the southern Great Plains in Spring. Part I: Structure, dynamics and seasonal evolution. *Wea. Forecasting*, **6**, 181–197.

Lanicci, J. M. and T. T. Warner, 1997: A case study of lid evolution using analyses of observational data and a numerical model simulation. *Wea. Forecasting*, **12**, 228–252.

MESO Inc., 1993: *MASS Version 5.8 Reference Manual*. (Available from MESO Inc., 185 Jordan Road, Troy, NY 12180).

Pfeiffer, K. D., M. L. Kaplan, Y.-L. Lin, A. J. Riordan, G. M. Lackmann, K. T. W. III, and D. B. Ensley, 2001a: The mesoscale evolution of the March 1993 Storm of the Century. Part I: Origin of the precursor convective available potential energy. Submitted to *Mon. Wea. Rev.*, May 2001.

Pfeiffer, K. D., M. L. Kaplan, Y.-L. Lin, A. J. Riordan, G. M. Lackmann, K. T. W. III, and D. B. Ensley, 2001b: The mesoscale evolution of the March 1993 Storm of the Century. Part II: Initiation and maintenance of antecedent deep convection. Submitted to *Mon. Wea. Rev.*, May 2001.

Uccellini, L. W., P. J. Kocin, R. S. Schneider, P. M. Stokels, and R. A. Dorr, 1995: Forecasting the 12–14 March Superstorm. *Bull. Amer. Meteor. Soc.*, **76**, 183–199.

Zeigler, C. L. and C. E. Hane, 1993: An observational study of the dryline. *Mon. Wea. Rev.*, **121**, 1134–1151.